Syntheses, Characterization, and Structural Studies of Several (Nitro)(nitrosyl)iron(III) Porphyrinates: [Fe(Porph)(NO_2)(NO)]

Mary K. Ellison,[†] Charles E. Schulz,*[,‡] and W. Robert Scheidt*[,†]

The Department of Chemistry and Biochemistry, University of Notre Dame, Notre Dame, Indiana 46556, and Department of Physics, Knox College, Galesburg, Illinois 61401

Received October 1, 1998

The preparation and characterization of several (nitro)(nitrosyl)iron(III) complexes, [Fe(Porph)(NO_2)(NO)], where Porph = tetraphenylporphyrin, octaethylporphyrin, tetra-*p*-methoxyphenylporphyrin, or picket fence porphyrin, are described. Crystal data: [Fe(T*p*-OCH_3PP)(NO_2)(NO)]·CH_2Cl_2, tetragonal, space group $I4_1/a$, $Z = 4$, with $a = 15.620(3)$ Å, $c = 18.649(2)$ Å; [Fe(TpivPP)(NO_2)(NO)]·C_6H_5Cl (**1**), tetragonal, $P4/ncc$, $Z = 4$, with $a = 18.094(3)$ Å, $c = 18.939(4)$ Å, and (**2**) with $a = 18.117(2)$ Å, $c = 19.0838(8)$ Å; [Fe(TpivPP)(NO_2)(NO)] (**3**), monoclinic, $C2/c$, $Z = 2$, with $a = 16.1559(5)$ Å, $b = 18.6920(8)$ Å, $c = 19.7779(10)$ Å, and $\beta = 90.971(6)°$; [Fe(TpivPP)(NO_2)(NO)]·C_7H_8 (**4**), monoclinic, $P2_1/n$, $Z = 4$, with $a = 12.7764(10)$ Å, $b = 27.192(2)$ Å, $c = 19.1716(8)$ Å, and $\beta = 105.063(5)°$. Of the several crystal structures described, two (out of four characterized) picket fence porphyrin derivatives exhibited no crystallographic disorder that led to problems defining the axial ligand geometry. In these two derivatives the Fe−axial ligand distances are Fe−N(NO) = 1.668(2) or 1.671(2) Å and Fe−N(NO_2) = 2.002(2) or 1.998(2) Å; NO does not cause a significant structural trans effect. The average Fe−N_p distance of 1.998(4) Å is consistent with a low-spin state for iron. The linear or near-linear (169.3(2)°) Fe−N−O angle observed is that expected for {FeNO}^{6} (i.e., iron(III) nitrosyl) species. The solid-state NO stretching frequencies (1871−1893 cm^{-1}) are also consistent with a linear Fe−N−O group. Mössbauer spectra show that the complexes have quadrupole splittings $\Delta E_q = 1.35-1.50$ mm/s and isomer shifts $\delta = 0.0-0.11$ mm/s; the isomer shifts display a strong temperature dependence with lower values at high temperature. Mössbauer spectra in applied magnetic field at 4.2 K show that the molecules have diamagnetic ground states which is presumed to result from antiferromagnetic coupling between the low-spin iron(III) and the $S = {}^1/_2$ nitric oxide center.

Introduction

The discovery that mammalian cells produce nitric oxide (NO) has led to a resurgence of interest in this molecule in many areas of science. New interactions of NO in biological systems are being discovered at a rapid rate. NO is found to be a crucial molecule in many important regulatory functions such as neurotransmission, blood pressure regulation, inhibition of platelet aggregation, and cytotoxic action of macrophages.[1] Many of the mammalian responses result from the interaction of NO with the ferrous heme of soluble guanylate cyclase. Recently, however, ferric nitrosyl heme proteins were found to be involved in fungal and bacterial denitrification processes.[2,3] Heme nitrite species are also possible intermediates in these denitrification processes especially in the enzyme nitrite reductase. Moreover, iron(III) hemes, which reversibly bind NO, have been discovered in the salivary glands of the bloodsucking insects *Rhodnius prolixus* and *Cimex lectularius*.[4,5] These heme proteins release NO in host tissues causing local vasodilation, which aids the bug's blood feeding.

Studies of the interaction of the ligands NO and/or NO_2^- ion with transition metal complexes, especially metalloporphyrins, have been and are expected to continue to be important in understanding their properties and the basis for the biological processes in which they play important roles. Over the years, we have synthesized and characterized a number of iron(II) and iron(III) porphyrin complexes in which either NO or NO_2^- is an axial ligand.[6−14] We have recently reported the synthesis, structures, and physical properties of two forms of the mixed-ligand, six-coordinate iron(II) complex [Fe(TpivPP)(NO_2)(NO)]$^-$.[15,16] The two crystalline forms differ most prominently

* To whom correspondence should be addressed.
[†] University of Notre Dame.
[‡] Knox College.

(1) (a) Butler, A. R.; Williams, D. L. H. *Chem. Soc. Rev.* **1993**, 233. (b) Stamler, J. S.; Singel, D. J.; Loscalzo, J. *Science* **1992**, *258*, 1898. (c) Yu, A. E.; Hu, S.; Spiro, T. G.; Burstyn, J. N. *J. Am. Chem. Soc.* **1994**, *116*, 4117. (d) Ignarro, L. J. *Circ. Res.* **1989**, *65*, 1. (e) Moncada, S.; Palmer, R. M. J.; Higgs, E. A. *Pharmacol. Rev.* **1991**, *43*, 109.
(2) Obayashi, E.; Tsukamoto, K.; Adachi, S.; Takahashi, S.; Nomura, M.; Iizuka, T.; Shoun, H.; Shiro, Y. *J. Am. Chem. Soc.* **1997**, *119*, 7807.
(3) Averill, B. A. *Chem. Rev.* **1996**, *96*, 2951 and references therein.
(4) (a) Ribeiro, J. M. C.; Hazzard, J. M. H.; Nussenzveig, R. H.; Champagne, D. E.; Walker, F. A. *Science* **1993**, *260*, 539. (b) Anderson, J. F.; Champagne, D. E.; Weichsel, A.; Ribeiro, J. M. C.; Balfour, C. A.; Dress, V.; Montfort, W. R. *Biochemistry* **1997**, *36*, 4423.
(5) Valenzuela, J. G.; Walker, F. A.; Ribeiro, J. M. C. *J. Exp. Biol.* **1995**, *198*, 1519.
(6) Scheidt, W. R.; Frisse, M. E. *J. Am. Chem. Soc.* **1975**, *97*, 17.
(7) Piciulo, P. L.; Scheidt, W. R. *J. Am. Chem. Soc.* **1976**, *98*, 1913.
(8) Scheidt, W. R.; Brinegar, A. C.; Ferro, E. B.; Kirner, J. F. *J. Am. Chem. Soc.* **1977**, *99*, 7315.
(9) Scheidt, W. R.; Lee, Y. J.; Hatano, K. *J. Am. Chem. Soc.* **1984**, *106*, 3191.
(10) Ellison, M. K.; Scheidt, W. R. *J. Am. Chem. Soc.* **1997**, *119*, 7404.
(11) Nasri, H.; Goodwin, J. A.; Scheidt, W. R. *Inorg. Chem.* **1990**, *29*, 185.
(12) Nasri, H.; Wang, Y.; Huynh, B. H.; Scheidt, W. R. *J. Am. Chem. Soc.* **1991**, *113*, 717.
(13) Nasri, H.; Wang, Y.; Huynh, B. H.; Walker, F. A.; Scheidt, W. R. *Inorg. Chem.* **1991**, *30*, 1483.
(14) Nasri, H.; Haller, K. J.; Wang, Y.; Huynh, B. H.; Scheidt, W. R. *Inorg. Chem.* **1992**, *31*, 3459.

10.1021/ic981162n CCC: $18.00
Published on Web 12/16/1998

in having different relative axial ligand orientations. In the two forms, the planes defined by the axial ligand NO_2^- and the nitrosyl Fe−N−O plane have either relative perpendicular or parallel orientations. The two different ligand orientations have an effect on the electronic structure at iron as shown by Mössbauer spectroscopy. The form with relative perpendicular ligand planes maximizes the π bonding since each of the two ligands interacts with a distinct iron d_π orbital while in the parallel form the two coplanar ligands are competing for π bonding. In both forms, a significant increase in the Fe−N(NO_2) bond distance trans to NO is observed (compared to either the five-coordinate species $[Fe(TpivPP)(NO_2)]^-$ [12] or six-coordinate derivatives[17]).

Despite the progress made with iron(II) derivatives, there is a limited amount of structural and physical data on iron(III) nitrosyl porphyrin derivatives. Herein we report the synthesis, characterization, and structural studies on the iron(III) (nitro)-(nitrosyl) complexes analogous to the iron(II) derivatives described above. These studies show the importance of the π interaction between iron and the axial ligands. The iron(III) (nitro)(nitrosyl) TPP, OEP, and PPIXDME complexes have been previously studied;[18,19] these were primarily solution studies, and no crystalline solids were obtained. Ruthenium derivatives with the same ligand set have been isolated and characterized,[20] but the nature of the coordinated NO_2^- in the ruthenium species differs significantly from the iron systems.

Experimental Section

General Information. Chlorobenzene was purified by washing with sulfuric acid and then distilled over P_2O_5. Methylene chloride and chloroform were distilled over CaH_2. Toluene and hexanes were distilled over sodium benzophenone. NO gas was purified by passing it through 4 Å molecular sieves immersed in a dry ice/ethanol slush bath to remove higher oxides of nitrogen.[21] H_2OEP was purchased from Midcentury Chemicals. All other chemicals were used as received from Aldrich or Fisher. Reactions involving addition of NO were done using standard Schlenkware techniques. IR spectra were recorded on a Perkin-Elmer 883 IR spectrophotometer as Nujol mulls; electronic spectra were recorded on a Perkin-Elmer Lambda 19 UV/vis/near-IR spectrometer. The solid-state Mössbauer samples were immobilized in Apiezon grease. The free bases, H_2TPP and H_2T*p*-OCH_3PP, were prepared according to Adler et al.[22] [Fe(Porph)Cl] was prepared according to a modified Adler preparation.[23] $[Fe(Porph)]_2O$ was prepared from [Fe-(Porph)Cl].[24] H_2TpivPP and the corresponding iron(III) chloro and triflate derivatives were synthesized by literature methods.[25,26] [K(18-C-6)(H_2O)][Fe(NO_2)$_2$(TpivPP)] and [Fe(TpivPP)(NO)] were also prepared by literature methods.[6,11]

Preparation of [Fe(Porph)(NO_2)(NO)]. The TPP, OEP, and T*p*-OCH_3PP complexes were prepared according to Settin and Fanning[18,27] with modifications to obtain X-ray-quality crystals. To 16 mg of $[Fe(TPP)]_2O$ was added 5 mL of $CHCl_3$. To 22 mg of $[Fe(OEP)]_2O$ was added 6 mL of toluene. To 25 mg of $[Fe(Tp\text{-}OCH_3PP)]_2O$ were added 8 mL of C_6H_5Cl and 2 mL of CH_2Cl_2. The solutions were degassed by argon purge, and then NO gas was bubbled in slowly for 30 min. There is a dramatic color change from green to red/orange, and the reactions were thought to be complete upon disappearance of the green color. X-ray-quality crystals were obtained by liquid diffusion using hexanes as the nonsolvent. IR (Nujol) (TPP, OEP, T*p*-OCH_3-PP): ν(NO) 1877, 1883, 1871 cm^{-1}. UV−vis (TPP, CH_2Cl_2), 431, 544, 578 (sh), 615 nm; (OEP, CH_2Cl_2), 415, 528, 560 nm; (T*p*-OCH_3PP, C_6H_5Cl), 437, 549, 586 nm.

Preparation of [Fe(TpivPP)(NO_2)(NO)]. Method IA.[19] A 20 mg amount of [Fe(TpivPP)(NO)] was dissolved in 7 mL of C_6H_5Cl or toluene (Method **IB**). NO was bubbled into the solutions for 30 min. The color changes slightly from red to orange-red. X-ray-quality crystals were obtained by liquid diffusion in sealed 8 mm glass tubes using hexanes as the nonsolvent (**IA**) or, subsequently, by vapor diffusion under an NO atmosphere using a 1:1 toluene/hexanes mixture as the nonsolvent (**IB**).

Method II. A 20 mg amount of [K(18-C-6)(H_2O)][Fe(NO_2)$_2$-(TpivPP)] was dissolved in 8 mL of C_6H_5Cl. NO was bubbled into this solution for 30 min. The color of the solution changes only slightly. X-ray-quality crystals were obtained by liquid diffusion using hexanes as the nonsolvent. IR (Nujol) (**IA**, **IB**, **II**): ν(NO) = 1873, 1893, 1893 cm^{-1}. IR (CH_2Cl_2, C_7H_8) (**IB**): ν(NO) = 1891, 1882 cm^{-1}. UV−vis (toluene): 433, 543 nm.

X-ray Structure Determinations. All structure determinations were carried out on an Enraf-Nonius FAST area-detector diffractometer with a Mo rotating anode source ($\bar{\lambda}$ = 0.710 73 Å). Our detailed methods and procedures for small-molecule X-ray data collection with the FAST system have been described previously.[28] Data collections were performed at 130(2) K. The structures were solved using the direct methods program SHELXS-86;[29] subsequent difference Fourier syntheses led to the location of most of the remaining nonhydrogen atoms. The structures were refined against F^2 with the program SHELXL-93,[30,31] in which all data collected were used including negative intensities. Hydrogen atoms of the porphyrin ligand and the solvent molecules were idealized with the standard SHELXL-93 idealization methods. A modified[32] version of the absorption correction program DIFABS was applied. Brief crystal data are listed in Table 1. Complete crystallographic details for the completed structures are included in the Supporting Information.

(15) Nasri, H.; Ellison, M. K.; Chen, S.; Huynh, B. H.; Scheidt, W. R. *J. Am. Chem. Soc.* **1997**, *119*, 6274.

(16) Abbreviations: Porph, a generalized porphyrin dianion; OEP, TPP, T*p*-OCH_3PP, TpivPP, PPIXDME, TMP, T*p*-ClPP, T(*p*-Me)PP, dianions of octaethylporphyrin, *meso*-tetraphenylporphyrin, *meso*-tetra-*p*-methoxyphenylporphyrin; (α,α,α,α-tetrakis(*o*-pivalamidophenyl)-porphyrin, protoporphyrin IX dimethyl ester, *meso*-tetramesitylporphyrin; *meso*-tetra-*p*-chlorophenylporphyrin, *meso*-tetra-*p*-methylphenylporphyrin; 18-C-6, 1,4,7,10,13,16-hexaoxacyclooctadecane (18-crown-6); N_p, porphyrinato nitrogen; N_{ax}, axial nitrogen; EPR, electron paramagnetic resonance; Pz, pyrazole; Iz, indazole (benzopyrazole); Prz, pyrazine; Py, pyridine; *t*-BuNC, *t*-butyl isocyanide; 2-MeHIm, 2-methylimidazole; 3-EtPy, 3-ethylpyridine; 3-ClPy, 3-chloropyridine; 4-NMe_2Py, 4-(dimethylamino)pyridine; 1,2-Me_2Im, 1,2-dimethylimidazole; 4-CNPy, 4-cyanopyridine; 1-MeIm, 1-methylimidazole; HIm, imidazole; CCP, cytochrome *c* peroxidase; Mb, myoglobin.

(17) Nasri, H.; Scheidt, W. R., manuscript in preparation.

(18) Settin, M. F.; Fanning, J. C. *Inorg. Chem.* **1988**, *27*, 1431.

(19) Yoshimura, T. *Inorg. Chim. Acta* **1984**, *83*, 17.

(20) (a) Fajer, J., personal communication. (b) Kadish, K. M.; Adamian, V. A.; Van Caemelbecke, E.; Tan, Z.; Tagliatesta, P.; Bianco, P.; Boshi, T.; Yi, G.-B.; Khan, M.; Richter-Addo, G. B. *Inorg. Chem.* **1996**, *35*, 1343. (c) Bohle, D. S.; Gopodson, P. A.; Smith, B. D. *Polyhedron* **1996**, *15*, 3147. (d) Miranda, K. M.; Bu, X.; Lorković, I.; Ford, P. C. *Inorg. Chem.* **1997**, *36*, 4838.

(21) Dodd, R. E.; Robinson, P. L. *Experimental Inorganic Chemistry*; Elsevier: New York, 1957; pp 233−234.

(22) Adler, A. D.; Longo, F. R.; Finarelli, J. D.; Goldmacher, J.; Assour, J.; Korsakoff, L. *J. Org. Chem.* **1967**, *32*, 476.

(23) (a) Adler, A. D.; Longo, F. R.; Kampus, F.; Kim, J. *J. Inorg. Nucl. Chem.* **1970**, *32*, 2443. (b) Buchler, J. W. In *Porphyrins and Metalloporphyrins*; Smith, K. M., Ed.; Elsevier Scientific Publishing: Amsterdam, The Netherlands, 1975; Chapter 5.

(24) (a) Fleischer, E. B.; Srivastava, T. S. *J. Am. Chem. Soc.* **1969**, *91*, 2403. (b) Hoffman, A. B.; Collins, D. M.; Day, V. W.; Fleischer, E. B.; Srivastava, T. S.; Hoard, J. L. *J. Am. Chem. Soc.* **1972**, *94*, 3620.

(25) Collman, J. P.; Gagne, R. R.; Halbert, T. R.; Lang, G.; Robinson, W. T. *J. Am. Chem. Soc.* **1975**, *97*, 1427.

(26) Gismelseed; A.; Bominaar, E. L.; Bill, E.; Trautwein, A. X.; Nasri, H.; Doppelt, P.; Mandon, D.; Fischer, J.; Weiss, R. *Inorg. Chem.* **1992**, *31*, 1845.

(27) This method was independently also discovered in our laboratory by Juchang Kim.

(28) Scheidt, W. R.; Turowska-Tyrk, I. *Inorg. Chem.* **1994**, *33*, 1314.

(29) Sheldrick, G. M. *Acta Crystallogr.* **1990**, *A46*, 467.

(30) Sheldrick, G. M. *J. Appl. Crystallogr.*, in preparation.

(31) $R1 = \sum||F_o| - |F_c||/\sum|F_o|$ and $wR2 = \{\sum[w(F_o^2 - F_c^2)^2]/\sum[wF_o^4]\}^{1/2}$. The conventional *R* factors R1 are based on *F*, with *F* set to zero for negative F^2. The criterion of $F^2 > 2\sigma(F^2)$ was used only for calculating R1. *R* factors based on F^2 (wR2) are statistically about twice as large as those based on *F*, and *R* factors based on *all* data will be even larger.

Table 1. Crystallographic Details for [Fe(Porph)(NO_2)(NO)] Derivatives at 130(2) K[a]

porphyrin	TPP	OEP	T*p*-OCH_3PP	TpivPP (**1**)	TpivPP (**2**)	TpivPP (**3**)	TpivPP (**4**)
syn. method[b]	μ-oxo	μ-oxo	μ-oxo	**IA**	**II**	**II**	**IB**
formula	$[Fe(N_4C_{44}H_{28})(NO_2)(NO)]$	$[Fe(N_4C_{36}H_{44})(NO_2)(NO)]$	$[Fe(O_4N_4C_{48}H_{36})(NO_2)(NO)]\cdot(CH_2Cl_2)$	$[Fe(O_4N_8C_{64}H_{64})(NO_2)(NO)]\cdot(C_6H_5Cl)$		$\cdot(C_7H_8)$	
fw	744.58	664.62	949.60	1253.65		1141.10	1233.24
a, Å	13.552(2)	13.5681(8)	15.620(3)	18.094(3)	18.117(2)	16.1559(5)	12.7764(10)
b, Å						18.6920(8)	27.192(2)
c, Å	9.656(2)	8.5155(8)	18.649(2)	18.939(4)	19.0838(8)	19.7779(10)	19.1716(8)
β, deg						90.971	105.063(5)
V, Å^3	1773.3	1567.6	4549.8(14)	6200.5(18)	6263.9(8)	5971.8(4)	6431.7(7)
Z	2	2	4	4	4	4	4
space group	*I*4/*m*	*I*4/*m*	$I4_1/a$	*P*4/*ncc*	*P*4/*ncc*	*C*2/*c*	$P2_1/n$
Fe site symmetry	4/*m*	4/*m*	$\bar{4}$	4	4	2	1
D_c, g/cm^3	1.394	1.408	1.386	1.343	1.329	1.269	1.274
μ, mm^{-1}	0.48	0.53	0.508	0.351	0.347	0.314	0.297
final *R* indices [I > 2 σ (I)]			R1 = 0.0592, wR2 = 0.1539	R1 = 0.0888, wR2 = 0.2147	R1 = 0.0901, wR2 = 0.1896	R1 = 0.0469, wR2 = 0.1174	R1 = 0.0477, wR2 = 0.1078
final *R* indices [for all data]			R1 = 0.0855, wR2 = 0.1818	R1 = 0.1178, wR2 = 0.2371	R1 = 0.1038, wR2 = 0.1956	R1 = 0.0582, wR2 = 0.1270	R1 = 0.0625, wR2 = 0.1154

[a] All data collected with Mo Kα radiation; $\bar{\lambda}$ = 0.710 73 Å. [b] Method of preparation (see Experimental Section).

Dark-purple, square-pyramidal crystals of [Fe(TPP)(NO_2)(NO)] (0.30 × 0.30 × 0.10 mm^3), [Fe(OEP)(NO_2)(NO)] (0.20 × 0.20 × 0.05 mm^3), and [Fe(T*p*-OCH_3 PP)(NO_2)(NO)]·CH_2Cl_2 (0.40 × 0.40 × 0.30 mm^3), were used for the structure determinations. Disorder caused by crystallographically required symmetry in the TPP and OEP case resulted in structures deemed not worthy of completion. In the T*p*-OCH_3PP case, there is one disordered methylene chloride per unit cell. Two components, with occupancy coefficients 0.20 and 0.05, share one chlorine atom. The two are related to three other pairs by a $\bar{4}$ symmetry operator. All non-hydrogen atoms, except the oxygen atom of the nitrosyl ligand, the chlorine atom of the minor component, and the carbon atoms of both components of the methylene chloride solvent, were refined anisotropically.

Synthetic method **I** produced two types of crystals depending on the solvent used in the crystallization. A rectangular block of [Fe(TpivPP)(NO_2)(NO)] (**1**) (0.40 × 0.30 × 0.06 mm^3) and a rhombohedron of [Fe(TpivPP)(NO_2)(NO)] (**4**) (0.30 × 0.30 × 0.20 mm^3 cut from a larger crystal) were used for the structure determinations. In the block crystal there is disorder in the axial ligands. There is a refined 57% occupancy of a linear nitrosyl on the picket side of the porphyrin face and a nitro ligand on the open face. The remaining 43% is [Fe^{II}(TpivPP)(NO)] represented by a bent nitrosyl bound to the open face. The *t*-butyl group of the picket occupies two positions with refined isotropic occupancies of 0.61 and 0.39. The carbonyl oxygen also occupies two positions refined to be 0.53 and 0.47. A rigid body refinement was used to locate the molecule of C_6H_5Cl that is disordered around a $\bar{4}$ axis. In [Fe(TpivPP)(NO_2)(NO)] (**4**), the toluene solvent molecule was disordered over two overlapping positions but was otherwise completely ordered. A rigid body refinement, using the major toluene component as a model, was used to define the minor component. This constraint was used in the early stages and was released near the end of the refinement. The occupancy of the major component was assigned to be 0.80, and the minor component 0.20. Synthetic method **II** produced rectangular blocks and rhombohedrons from the same crystallization experiment. A block (0.43 × 0.33 × 0.27 mm^3) and a rhomb (0.53 × 0.40 × 0.30 mm^3 cut from a larger crystal) were used for the structure determinations. The block crystal, examined first, is [Fe(TpivPP)(NO_2)(NO)] (**2**) which is isomorphous with the blocks obtained in Method **I**. There is an in/out-of-pocket disorder of the axial ligands. The nitro group has a refined occupancy of 74% in the pocket and 26% out of the pocket with respective opposite occupancies of the nitrosyl group. The *t*-butyl group of one picket occupies two positions with refined occupancies of 0.57 and 0.43. The rhombs are unsolvated [Fe(TpivPP)(NO_2)(NO)] (**3**) with crystallographically required 2-fold symmetry perpendicular to the porphyrin plane.

(32) The process is based on an adaptation of the DIFABS[33] logic to area detector geometry by A. I. Karaulov: School of Chemistry and Applied Chemistry, University of Wales, College of Cardiff, Cardiff CF1 3TB, U.K., personal communication.

Table 2. Summary of Structural Results for [Fe(Porph)(NO_2)(NO)]

porphyrin	ν(NO) (cm^{-1})[a]	result, Fe site symmetry, metrical usefulness[b]
TPP	1877	severe disorder, 4/*m*, none
OEP	1883	severe disorder, 4/*m*, none
T*p*-OCH_3PP	1871	major disorder, $\bar{4}$, limited
TpivPP (**1**)	1873, 1893(sh)	major disorder (mixture), 4, none
TpivPP (**2**)	1893	minor in/out disorder, 4, moderate
TpivPP (**3**)	1893	ordered, 2, substantial
TpivPP (**4**)	1893	ordered, 1, complete
	1891,[c] 1882[d]	

[a] Nujol mull. [b] Metrical usefulness refers specifically to the characterization of the axial bond distances and angles. [c] CH_2Cl_2 solution. [d] Toluene solution.

Results

Several crystalline (nitro)(nitrosyl) porphyrin species have been isolated and subjected to X-ray analysis as summarized in Table 2. The four picket fence derivatives ([Fe(TpivPP)(NO_2)(NO)]) are denoted as **1**, **2**, **3**, or **4**, as described in the Experimental Section and detailed in Table 1. Only two picket fence derivatives had completely ordered axial ligands, but a total of five crystalline derivatives gave some useful structural results; selected bond parameters for these derivatives are given in Table 3. Tables listing complete crystallographic details, atomic coordinates, bond distances and angles, anisotropic temperature factors, and fixed hydrogen atom positions are provided in the Supporting Information. Also included in the Supporting Information are formal diagrams of the porphyrin core displaying the average bond parameters and the displacement of the core atoms from the 24-atom mean plane (Figures S1−S4). ORTEP diagrams of [Fe(T*p*-OCH_3PP)(NO_2)(NO)], the major species in [Fe(TpivPP)(NO_2)(NO)] (**1**), and both in/out-of-pocket isomers in [Fe(TpivPP)(NO_2)(NO)] (**2**) are also included in the Supporting Information (Figures S5−S7).

ORTEP diagrams of [Fe(TpivPP)(NO_2)(NO)] (**3** and **4**) are given in Figures 1 and 2. Completely labeled diagrams are included in the Supporting Information (Figures S8 and S9). There is a 2-fold axis of symmetry perpendicular to the porphyrin plane in **3** that requires the nitrosyl ligand to be exactly linear; there is no required symmetry in **4**. The labeling schemes displayed in Figures 1 and S9 and in Figures S5−S7 are those used in the respective diagrams and tables. Figure 3, a formal diagram of the porphinato core of [Fe(TpivPP)(NO_2)(NO)] (**4**), displays the averaged bond parameters found in that derivative; values for the other derivatives are similar.

Table 3. Selected Bond Parameters for [Fe(Porph)(NO_2)(NO)]

complex	T*p*-OCH_3PP	TpivPP (**1**)	TpivPP (**2**)	TpivPP (**3**)	TpivPP (**4**)
Fe−N_p[a,b]	1.998(2)	1.991(2)	2.000(2)	2.000(5)	1.996(4)
Fe−N_{NO}[a]	1.85[c]	1.87[c]	1.733[c] [1.631][d]	1.668(2)	1.671(2)
Fe−N_{NO_2}[a]	1.85[c]	1.85[c]	1.916[c] [2.018][d]	2.002(2)	1.998(2)
O−N_{NO}[a]	1.14[c]	1.11[c]	1.107[c]	1.132(3)	1.144(3)
O−N_{NO_2}[a]	1.27[c]	1.20[c]	1.246[c]	1.226(2)	1.224(3), 1.222(3)
Fe−N−O[e]	160.2[c]	180.00	180.00	180.00	169.3(2)
O−N−O[e]	115.9[c]	114[c]	120.8(8)	120.8(2)	121.4(2)
ΔFe[a,f]	*c*	*c*	0.12	0.15	0.09
NO_2^- orient.[e,g]	42.3	43.8	43.5	41.0	44.1

[a] Value in ångstroms. [b] Averaged values for **3** and **4**. [c] Value obscured or likely affected by disorder. [d] Value calculated from population averages. Corrections calculated from the simultaneous equations: $1.733 = (\alpha)(Fe-N_{NO}) + (1-\alpha)(Fe-N_{NO_2})$ and $1.916 = (1-\alpha)(Fe-N_{NO}) + (\alpha)(Fe-N_{NO_2})$ where α = majority fraction (NO out-of-pocket; NO_2^- in-pocket) and refined to be 0.737. [e] Value in degrees. [f] All displacements toward NO. [g] Dihedral angle between NO_2 plane and closest N_{NO_2}−Fe−N_p coordinate plane.

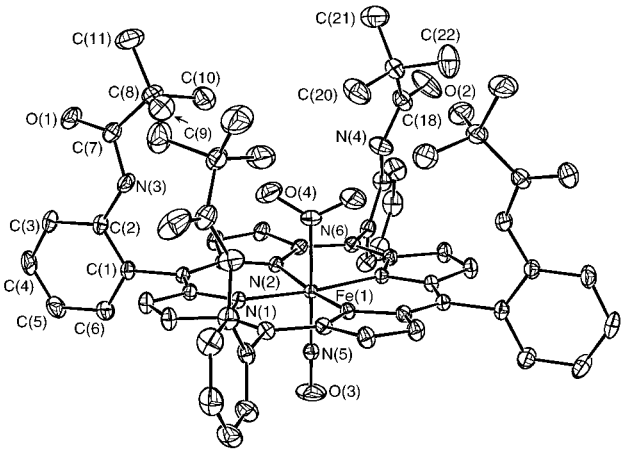

Figure 1. ORTEP diagram illustrating the molecular structure of [Fe(TpivPP)(NO_2)(NO)] (**3**) (50% probability ellipsoids). Selected labels of the crystallographically unique atoms are shown. The crystallographic 2-fold axis is along the N(6)−Fe(1)−N(5)−O(1) bond system.

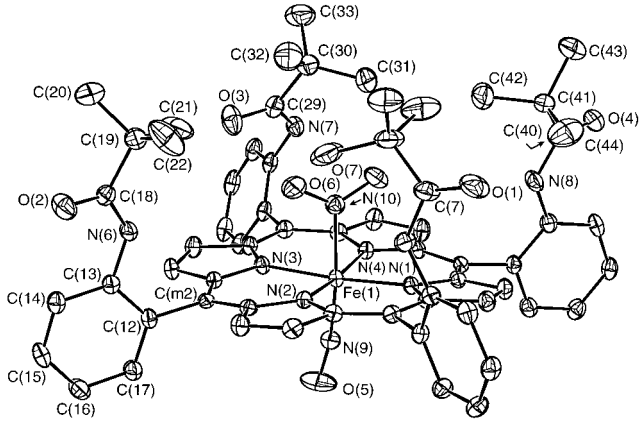

Figure 2. ORTEP diagram illustrating the molecular structure and selected labels of [Fe(TpivPP)(NO_2)(NO)] (**4**) (50% probability ellipsoids).

Table 2 also lists the NO stretching frequencies for the isolated crystalline solids. The picket fence complex with NO predominantly in the pocket is 20 cm^{-1} lower than that of the other picket fence derivative where the NO is out of the pocket. The IR spectra obtained by dissolving solid [Fe(TpivPP)(NO_2)(NO)] (**4**) (obtained from Method **IB**) in CH_2Cl_2 or toluene reveals a single nitrosyl band with a small solvent-dependent shift. The UV−vis spectra for all of the (nitro)(nitrosyl) species show similar shifts; for each type, the Soret band is red-shifted relative to other corresponding low-spin iron(III) species.

Mössbauer measurements were made at 293 and 4.2 K for several of the (nitro)(nitrosyl) complexes. Two of the compounds were measured in a 7 T applied field at 4.2 K. The Mössbauer data are discussed subsequently.

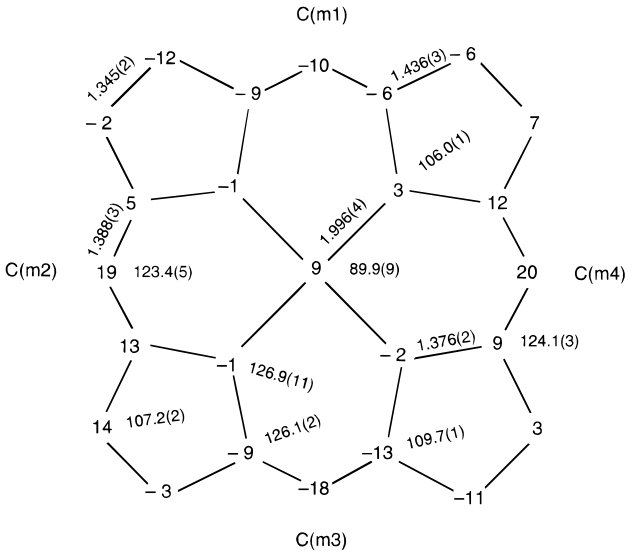

Figure 3. Formal diagram of the porphinato core of [Fe(TpivPP)(NO_2)(NO)] (**4**) illustrating the labeling scheme and the displacement of each unique atom from the mean plane of the 24-atom porphinato core. Also displayed on the diagram are the averaged values of each type of bond distance and angle in the porphinato core.

Discussion

Syntheses. Several (nitro)(nitrosyl)(porphinato)iron(III) complexes have been prepared and structurally characterized. The TPP, OEP, and T*p*-OCH_3PP derivatives were prepared by reaction of NO with the respective μ-oxoiron(III) porphyrin in a variety of solvents.[18,27] As described below, unsatisfactory crystallographic results for these derivatives led to the syntheses and characterization of picket fence porphyrin derivatives. It is to be emphasized that all synthetic procedures most probably lead to solutions containing a number of different nitrogen oxide ligand−iron species.

Scheme 1 shows two synthetic strategies that we have used to prepare picket fence porphyrin derivatives. Method **I** is based on the report that a (nitro)(nitrosyl)(porphinato)iron(III) complex can be made in solution starting with [Fe(TPP)(NO)].[19] However, for TPP, equilibration of the starting five-coordinate nitrosyl and the (nitro)(nitrosyl) was observed, no solid was isolated, and the possible intermediates in the reaction are not known. If the initial, transient species formed is a bis(nitrosyl) complex, with subsequent reaction to the (nitro)(nitrosyl)(porphinato)iron(III) complex, then starting with [Fe(TpivPP)(NO)], the method might be expected to provide the isomer in

Scheme 1. Proposed Synthetic Strategy for Obtaining Two Isomers of [Fe(TpivPP)(NO_2)(NO)]

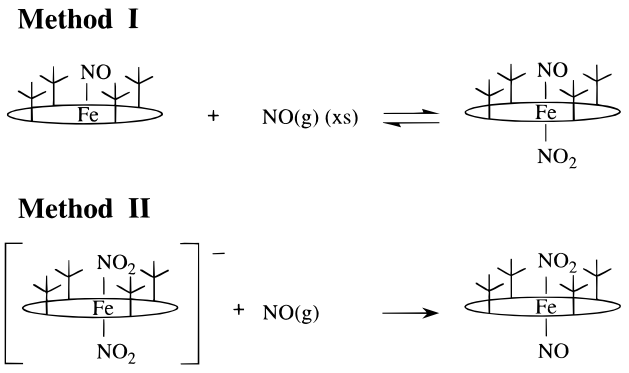

which the nitrosyl ligand is in the pocket and the nitro group is out of the pocket. This expectation is based on the idea that the ligand binding pocket would limit the reaction of the bis(nitrosyl) to the open face. Although this reaction, run in C_6H_5Cl, does produce the expected isomer of [Fe(TpivPP)(NO_2)(NO)], both the isolated bulk product and the single crystal are a mixture of the desired (nitro)(nitrosyl) complex and the five-coordinate nitrosyl derivative. Indeed, we have been unable to produce a pure sample of [Fe(TpivPP)(NO_2)(NO)] with nitrite out of the pocket. When this reaction was performed in toluene, a single isomer ([Fe(TpivPP)(NO_2)(NO)] (**4**)) was obtained but with the nitrite ion entirely in the ligand binding pocket.

Method **II** (Scheme 1) involves the reaction of the bis(nitro)iron(III) complex, [K(18-C-6)(H_2O)][Fe(TpivPP)(NO_2)$_2$], with NO. It was expected that NO would simply displace the exposed nitro ligand to yield the isomer in which the remaining nitro group is in the picket fence pocket. This reaction has been observed when the displacing ligand was pyridine,[13] imidazole,[13] or thiolate.[14] This expected result has largely been confirmed. Thus, although the strategies of Scheme 1 appear generally meritorious, the results are tempered by an apparent, solvent-dependent placement of the two axial ligands with the anion in the pocket the favored species. The in/out-of-pocket location of the axial ligands appears to be defined in the initial reaction and not by isomerization after product formation.[34] Finally, it may be noted that the position of the anionic nitrite ligand is consistent with the generally observed placement of an anionic ligand in the pocket for both five- and six-coordinate iron derivatives.

X-ray Structures. An important goal of the structural analyses of the mixed (nitro)(nitrosyl) complex was the accurate determination of the two axial bond distances, including the possible mutual effects on the distances. To finally achieve this goal, we have investigated seven different crystalline [Fe(Porph)(NO_2)(NO)] species by X-ray crystallography. A significant difficulty is the lack of differentiation in the solid state of the two comparably sized axial ligands. The near-equivalence of the two axial ligands leads to a crystallographically imposed symmetry that is too high for the molecule in the crystal and hence to structure determinations with limited metrical usefulness.

[Fe(TPP)(NO_2)(NO)] was the first complex studied. Its easy availability and the earlier reported spectroscopic data[18,19] made it a convenient choice. However, the complex crystallized in the tetragonal space group $I4/m$ with $Z = 2$ and required 4/m symmetry at iron, which prohibits any useful distinction between the two axial ligands. This is the result of the domination of the porphyrin ligand on the solid-state packing, a feature which has been noted previously for tetraarylporphyrins with small axial ligands.[20,35,36] The use of OEP as the porphyrin led to the same space group and disorder. This is somewhat surprising since Ford and co-workers have recently found that both [Ru(OEP)(NO)(ONO)] and [Ru(OEP)(NO)(OH)] have ordered axial ligands.[20d] The use of the aryl-substituted porphyrin Tp-OCH_3PP led to a crystalline species with required $\bar{4}$ site symmetry at iron. Although the overall structure is acceptable, the $\bar{4}$ iron site symmetry prevents any distinction between the two Fe−N_{ax} bond lengths. Interestingly, the closely related derivative [Co(Tp-OCH_3PP)(NO)] is observed to have only required 2-fold symmetry at cobalt.[37]

A drastic alteration of the porphyrin ligand appeared necessary to overcome the problem of high site symmetry and to allow differentiation of the two axial ligands. Picket fence porphyrin was a likely candidate but the previous synthetic strategy,[18] which used a μ-oxoiron(III) derivative as starting material, could not be used. As described earlier, two new synthetic methods to prepare crystalline [Fe(TpivPP)(NO_2)(NO)] were explored. The first crystalline complex was obtained using method **I** (Scheme 1) with chlorobenzene as the solvent. The structure of the predominant product is shown in Figure S6 of the Supporting Information. As we had expected, the synthetic method leads to the isomer with coordinated NO_2^- outside the ligand binding pocket and the nitrosyl ligand inside. While the synthetic method clearly provides [Fe(TpivPP)(NO_2)(NO)], the reaction solution and the isolated bulk solid contains [Fe(TpivPP)(NO)] as well, consistent with the solution equilibrium suggested by Yoshimura.[19] Although the predominant species in the crystal is the desired mixed ligand complex, five-coordinate [Fe(TpivPP)(NO)] was also present. Surprisingly, the nitrosyl ligand is outside the ligand binding pocket. Once again, the crystalline derivative does not provide adequate metrical data.

[Fe(TpivPP)(NO_2)(NO)] (**2** and **3**) were subsequently obtained using synthetic method **II** (Scheme 1, ligand displacement). The reaction was performed in chlorobenzene and crystals obtained directly from the reaction mixture. Two crystalline forms, both shown to be [Fe(TpivPP)(NO_2)(NO)], were noted during initial crystal examination. The first crystalline specimen selected led to the structural result shown in Figure S7 of the Supporting Information. Although the nitro ligand is found in the picket fence pocket as expected, there is an in/out-of-pocket disorder of the two axial ligands, with the nitro group predominantly, but not exclusively, in the pocket. However, the second crystalline form obtained from the reaction mixture has the expected, ordered arrangement of axial ligands as shown in Figure 1. In this form, the [Fe(TpivPP)(NO_2)(NO)] molecule has crystallographically required 2-fold symmetry perpendicular to the porphyrin plane which leads to a linear Fe−N−O group.

Finally, the use of the less polar solvent toluene in synthetic method **I** led to the preparation of a crystalline derivative with no required symmetry or crystallographic disorder. The structure of this derivative is shown in Figure 2. The arrangement of the

(33) Walker, N. P.; Stuart, D. *Acta Crystallogr., Sect. A* **1983**, *39*, 158.
(34) This is consistent with the appearance of a time-invariant single nitrosyl stretch in both CH_2Cl_2 and toluene.
(35) Scheidt, W. R.; Lee, Y. J. *Struct. Bonding (Berlin)* **1987**, *64*, 1.
(36) This phenomenon has been nicely exploited in a series of "programmable lattice clathrates;" see: Byrn, M. P.; Curtis, C. J.; Khan, S. I.; Sawin, P. A.; Tsurumi, R.; Strouse, C. *J. Am. Chem. Soc.* **1990**, *112*, 1865 and following papers.
(37) Richter-Addo, G. B.; Hodge, S. J.; Yi, G.-B.; Khan, M. A.; Ma, T.; Van Caemelbecke, E.; Guo, N.; Kadish, K. M. *Inorg. Chem.* **1996**, *35*, 6530; **1997**, *36*, 2696.

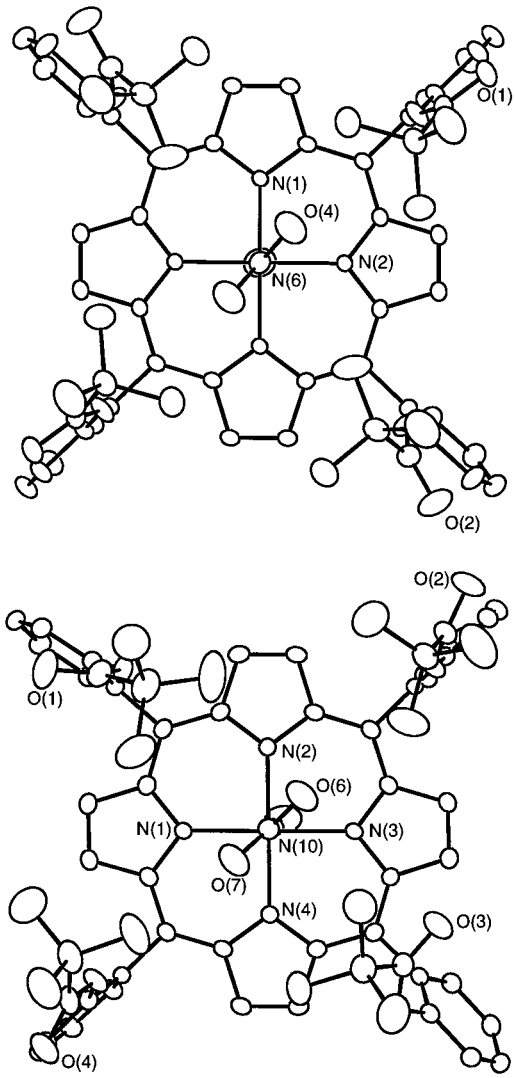

Figure 4. ORTEP diagrams illustrating the orientation of the nitrite ligand and the disposition of the pickets in (top) [Fe(TpivPP)(NO_2)(NO)] (**3**) and (bottom) [Fe(TpivPP)(NO_2)(NO)] (**4**). The plane of the porphyrin is parallel to the plane of the paper, and 50% probability ellipsoids are given.

two ordered axial ligands is opposite that initially expected from the synthetic procedure. However, the in/out-of-pocket arrangement conforms to the generally observed pattern in which a ligating anion, when present, is found in the pocket. Although the issue has not been explored rigorously, our in/out-of-pocket observations suggest that there is an inherent stability for the nitrite anion in the pocket and the nitrosyl ligand out of the pocket. This is accentuated by reactions in nonpolar solvents. Solution infrared spectra of this complex dissolved in CH_2Cl_2 or toluene do not suggest a slow isomerization of the axial ligands.

In all structures the N-bound nitro group is effectively perpendicular to the porphyrin mean plane. In some cases this feature is required by the crystallographic symmetry imposed on the molecule. In [Fe(TpivPP)(NO_2)(NO)] (**4**), with no imposed symmetry, the dihedral angle between the NO_2 plane and the 24-atom plane is 87.1°. Figure 4, a view normal to the porphyrin plane and looking into the pocket, shows the orientation of the nitro group with respect to Fe−N_p bonds in the porphyrin core. In both derivatives, the nitrite ion plane is close to bisecting an N_p−Fe−N_p angle (the actual values are 41.0 and 44.1°). Similar, near-bisecting, orientations of the nitro ligand were found in the other (nitro)(nitrosyl) derivatives of this study as well as earlier structural results on both iron(II) and iron(III) nitro complexes.[12−15,17] In earlier analyses of the Mössbauer spectra of nitrite complexes in applied magnetic field,[12,13] the necessity of rotating the $\tilde{g}$ and $\tilde{A}$ tensor axes with respect to the ligand field axes was noted. This somewhat unusual requirement was interpreted as the control of the orientation of the two d_π orbitals by the nitrite to an orientation between the Fe−N_p bond directions. The most reasonable explanation for such orbital orientation control is that the π bonding between nitrite and iron is more dominant than any possible π bonding between the porphyrin and iron.

Figure 4 also shows interesting features concerning the orientation of the amide and *t*-butyl group of the pickets that form the ligand binding pocket. The orientation of the *t*-butyl groups shown in [Fe(TpivPP)(NO_2)(NO)] (**3**) (top) illustrate the usual orientation of these groups with respect to the nitrite oxygen atoms. As is easily seen, each of the two oxygen atoms of nitrite are "cradled" by two methyl groups of the closest picket. This conformational feature is almost always the one seen in the structures of the known iron nitrite complexes.[13−15,17] It is not seen, however, for either oxygen atom of the nitrite in [Fe(TpivPP)(NO_2)(NO)] (**4**) (bottom). The significance of these specific nitrite oxygen atom−methyl group "interactions" is not known, but the preponderance of the "cradled" form suggests a small energetic preference for this conformation and which thus appears to be a molecular recognition feature. A second picket fence porphyrin conformational issue is also illustrated by the two molecules. It has generally been observed that the amide group is coplanar or nearly coplanar with its attached phenyl group; the N−H group of the picket is oriented toward the inside of the pocket. This is seen in all of the pickets of **3** and in three of the pickets in **4**. However, as is seen in Figure 4 (bottom), one amide group is not coplanar but has the amide oxygen atom tending to the inside and the N−H pointing away. The dihedral angle between the amide group and the phenyl is 112°.[38] Although this feature is unusual, it has been previously observed;[14,39] its cause remains obscure.

Table 3 gives selected structural parameters for the five [Fe(Porph)(NO_2)(NO)] structures. The range of averaged Fe−N_p bond lengths values is 1.991−2.000 Å; these are typical of low-spin iron(III) porphyrinates.[40] A low-spin state for the complexes could be expected since both five-coordinate [Fe(Porph)(NO)]$^{0+}$ complexes are known to be low spin.[15] [Fe(TpivPP)(NO_2)]$^-$ is also known to be low spin,[12] although the spin state of an iron(III) five-coordinate nitrite derivative has not yet been determined.[41] In all of the cases where it can be discerned, the iron is displaced slightly (0.09−0.15 Å) toward the nitrosyl ligand and toward the open face of the picket fence porphyrin. The displacement of iron toward the NO ligand reflects the stronger bonding between iron and NO.

When the Fe−N−O angle is not required by symmetry to be linear there are slight distortions from exact linearity observed. This angle is 160.2(6)° in the T*p*-OCH_3PP derivative and 169.3(2)° in the picket fence derivative. Small deviations

(38) It is to be noted that these dihedral angles are sometimes given as the angle between the phenyl group and the amide group without regard for the direction of the N−H vector. Hence, in the current case, the dihedral angle might have been given as its supplement (68°).

(39) (a) Baldacchini, C. J.; Groh, S. E.; Rheingold, A. L. *J. Inorg. Biochem.* **1990**, *36*, 161. (b) Munro, O. Q.; Scheidt, W. R. *Inorg. Chem.* **1998**, *37*, 2308.

(40) Scheidt, W. R.; Reed, C. A. *Chem. Rev.* **1981**, *81*, 543.

(41) Evidence that a five-coordinate iron(III) nitrite derivative is low spin comes from the EPR spectrum of a transient species; see: Munro, O. Q.; Scheidt, W. R. *Inorg. Chem.* **1998**, *37*, 2308.

Table 4. Coordination Group Bond Lengths for Nitro and/or Nitrosyl Derivatives

Fe(III) complex	Fe−N_p	Fe−$N(NO_2)$	Fe−N_{ax}	ref
$[Fe(TpivPP)(NO_2)_2]^-$	1.991(9)	1.970(5)	2.001(6)	11
$[Fe(TpivPP)(NO_2)(SC_5F_4H)]^-$	1.980(7)	1.990(7)	2.277(2)	14
$[Fe(TpivPP)(NO_2)(Py)]$	1.985(3)	1.960(5)	2.093(5)	13

	Fe−N_p	Fe−$N(NO_2)$	Fe−N_{NO}	ref
$[Fe(TpivPP)(NO_2)(NO)]$ (**2**)	2.000(2)	[2.018][a]	[1.631][a]	this work
$[Fe(TpivPP)(NO_2)(NO)]$ (**3**)	2.000(5)	2.002(2)	1.668(2)	this work
$[Fe(TpivPP)(NO_2)(NO)]$ (**4**)	1.996(4)	1.998(2)	1.671(2)	this work

	Fe−N_p	Fe−N_L	Fe−N_{NO}	ref
$[Fe(OEP)(NO)]^+$	1.994(1)	−	1.644(3)	9
$[Fe(TPP)(NO)(H_2O)]^+$	1.999(6)	2.001(5)	1.652(5)	9
$[Fe(TPP)(NO)(HO\text{-}i\text{-}C_5H_{11})]^+$	2.013(3)	2.063(3)	1.776(5)[b]	42
$[Fe(OEP)(Pz)(NO)]^+$	2.004(5)	1.988(2)	1.627(2)	43
$[Fe(OEP)(Iz)(NO)]^+$	1.996(4)	2.010(3)	1.632(3)	43
$\{[Fe(OEP)(NO)]_2Prz\}^{2+}$	1.995(8)	2.039(2)	1.632(3)	43

[a] Values corrected for disorder (see text and Table 3). [b] Reported value of N−O bond distance suggests that this distance is actually shorter.

from linearity, i.e., an off-axis position of the oxygen atom, are also suggested by the anisotropy of the temperature factors of the nitrosyl oxygen atoms in those derivatives required by symmetry to have a linear Fe−N−O group (cf. Figure 1). In the two derivatives for which there is no positional disorder of the axial ligands, the observed N−O bond lengths and O−N−O bond angles represent reasonable values for these parameters.

Table 4 lists the coordinating bond lengths for several nitro and/or nitrosyl iron(III) porphyrin derivatives. Values for three $[Fe(Porph)(NO_2)(NO)]$ derivatives are given in the middle section of the table. For $[Fe(TpivPP)(NO_2)(NO)]$ (**2**) a weighted average correction, based on the refined 74:26 in-pocket nitro/nitrosyl ratio, is given. The correction gives more appropriate axial ligand bond lengths that are initially obscured by the in/out disorder. The Fe−$N(NO_2)$ and Fe−N(NO) bond lengths reported for $[Fe(TpivPP)(NO_2)(NO)]$ (**3**) and $[Fe(TpivPP)(NO_2)(NO)]$ (**4**) are from completely ordered structures. The Fe−$N(NO_2)$ bond lengths in the (nitro)(nitrosyl) complexes are seen to be slightly longer than the Fe−$N(NO_2)$ bond lengths for the three $[Fe(TpivPP)(NO_2)(L)]$ complexes listed at the top of Table 4. Similarly, the Fe−N(NO) bond lengths in $[Fe(TpivPP)(NO_2)(NO)]$ (**3**) and $[Fe(TpivPP)(NO_2)(NO)]$ (**4**) also show small increases compared to the five- and six-coordinate iron(III) nitrosyl complexes given in the third group of Table 4. A likely origin for the small axial distance elongation is competition for iron π donation by the two axial ligands. There is, however, no significant trans effect for nitrosyl in the iron(III) complexes, in distinct contrast to the iron(II) nitrosyls. As noted earlier, the preparation of (nitro)(nitrosyl)(porphinato)ruthenium(III) complexes have been reported previously.[20] All ruthenium derivatives contain an O-bound NO_2^- ligand rather than the N-bound species observed for the iron complexes. The linkage isomer difference presumably reflects a greater importance of π bonding between the NO_2^- ligand and iron(III) than in the ruthenium complexes.

Physical Properties. The nitrosyl stretching frequencies for the several isolated species are listed in Table 2. The range of values is 1871−1893 cm^{-1}, consistent with that observed previously[18,19] and with the assignment of the complexes as containing a formal iron(III) center. The exact value of the stretching frequency shows some environmental effects; in particular, there is an apparent 20 cm^{-1} difference between the in/out-of-pocket nitrosyl derivatives. The observed NO frequencies are higher than that observed for five-coordinate $[Fe(OEP)(NO)]^+$ [9] and lower than that observed for six-coordinate species where the trans ligand is water,[9] alcohol,[42] or a neutral nitrogen donor.[43] The differences surely reflect the small, but real differences in iron π donation to the nitrosyl. The observed electronic spectra for all derivatives were similar to those seen earlier.[18,19]

The measurement of physical properties such as Mössbauer spectra and especially the magnetic susceptibility are made difficult by the problems of obtaining bulk products free from impurities. The most prominent impurity is the iron(II) nitrosyl that sometimes results from reductive nitrosylation. The possible presence of impurities in bulk samples was checked by EPR and IR spectroscopy. To ensure that there were no problems caused by a lack of long-term stability, all measurements were obtained on freshly prepared samples. Mössbauer spectra have been determined in zero applied field at various temperatures and in some cases in an applied magnetic field at 4.2 K; parameters for the (nitro)(nitrosyl) complexes are given at the top of Table 5. For all of the iron(III)(nitro)(nitrosyl) derivatives, one striking feature is the very low values of the isomer shift, which also displays a strong temperature dependence. For low-spin iron(III) species, the isomer shift values are typically much larger and display much smaller temperature dependences of the isomer shift than seen in the (nitro)(nitrosyl) complexes. Decreased values of the isomer shift are expected from increasing formal charge on iron; indeed an isomer shift near 0 mm/s is that expected for iron(IV) porphyrins.[55] The value of the quadrupole splitting is also somewhat unusual, with the values observed relatively small compared to most iron(III) porphyrinate species previously characterized. It should be noted that there is no effect of the position of the nitrosyl (in or out of the ligand binding pocket) on the Mössbauer spectral values. Table 5 details the observed isomer shifts and quadrupole splittings for a variety of low-spin iron(III) porphyrinates. In the data gathered are a number of compounds with relatively small values of the quadrupole splitting. For all of these species, small values of the quadrupole splitting are correlated with a degeneracy or a near-degeneracy of the d_{xz} and d_{yz} orbitals.[56] This is most easily seen and understood for the series of bis(planar axial ligand) complexes with relative perpendicular

(42) Yi, G.-B.; Chen, L.; Khan, M. A.; Richter-Addo, G. B. *Inorg. Chem.* **1997**, *36*, 3876.
(43) Ellison, M. K.; Scheidt, W. R., submitted for publication.
(44) Walker, F. A.; Nasri, H.; Turowska-Tyrk, I.; Mohanrao, K.; Watson, C. T.; Shokhirev, N. V.; Debrunner, P. G.; Scheidt, W. R. *J. Am. Chem. Soc.* **1996**, *118*, 12109.
(45) Safo, M. K.; Gupta, G. P.; Watson, C. T.; Simonis, U.; Walker, F. A.; Scheidt, W. R. *J. Am. Chem. Soc.* **1992**, *114*, 7066.
(46) Safo, M. K.; Gupta, G. P.; Walker, F. A.; Scheidt, W. R. *J. Am. Chem. Soc.* **1991**, *113*, 5497.
(47) Munro, O. Q.; Marques, H. M.; Debrunner, P. G.; Mohanrao, K.; Scheidt, W. R. *J. Am. Chem. Soc.* **1995**, *117*, 935.
(48) Safo, M. K.; Walker, F. A.; Raitsimring, A. M.; Walters, W. P.; Dolata, D. P.; Debrunner, P. G.; Scheidt, W. R. *J. Am. Chem. Soc.* **1994**, *116*, 7760.
(49) (a) Epstein, L. M.; Straub, D. K.; Maricondi, C. *Inorg. Chem.* **1967**, *6*, 1720. (b) Inniss, D.; Soltis, S. M.; Strouse, C. E. *J. Am. Chem. Soc.* **1988**, *110*, 5644.
(50) Scheidt, W. R.; Osvath, S. R.; Lee, Y. J.; Reed, C. A.; Shaevitz, B.; Gupta, G. P. *Inorg. Chem.* **1989**, *28*, 1591.
(51) Straub, D. K.; Conner, W. M. *Ann. N.Y. Acad. Sci.* **1973**, *206*, 383.
(52) Bohle, D. S.; Debrunner, P.; Fitzgerald, J.; Hansert, B.; Hung, C.-H.; Thompson, A. J. *J. Chem. Soc., Chem. Commun.* **1997**, 91−92.
(53) Pilard, M.-A.; Guillemot, M.; Toupet, L.; Jordanov, J.; Simonneaux, G. *Inorg. Chem.* **1997**, *36*, 6307.
(54) Rhynard, D.; Lang, G.; Spartalian, K.; Yonetani, T. *J. Chem. Phys.* **1979**, *71*, 3715.
(55) Debrunner, P. G. In *Iron Porphyrins*; Lever, A. B. P., Gray, H. B., Eds.; VCH Publishers Inc.: New York, 1983; Part 3, Chapter 2, Table 10.

Table 5. Mössbauer Parameters for the (Nitro)(Nitrosyl) Complexes and Related Derivatives

	ΔE_q, mm/s	δ_{Fe}, mm/s	T, K	ref
(nitro)(nitrosyl) Complexes				
[Fe(TPP)(NO_2)(NO)]	1.37	0.02	293	*a*
	1.36	0.13	4.2	*a*
	1.36	0.13	77	18
[Fe(T*p*-OCH_3PP)(NO_2)(NO)]	1.43	0.04	293	*a*
[Fe(TpivPP)(NO_2)$_{in}$(NO)$_{out}$]	1.48	0.01	293	*a*
	1.43	0.09	4.2	*a*
[Fe(TpivPP)(NO)$_{in}$(NO_2)$_{out}$]	1.50	0.00	293	*a*
Fe(III) Complexes				
[Fe(OEP)NO]ClO_4	1.63	0.12	293	*a*
	1.64	0.20	4.2	*a*
[Fe(TpivPP)(NO_2)$_2$]$^-$	2.1	0.25	4.2	13
[Fe(TpivPP)(NO_2)(Py)]	2.2	0.26	4.2	13
[Fe(TpivPP)(NO_2)(SC_6HF_4)]$^-$	2.12	0.22	293	14
	2.30	0.28	4.2	14
[Fe(OEP)(*t*-BuNC)$_2$]$^+$	1.67	0.08	300	44
	1.98	0.16	120	44
	2.06	0.18	4.2	44
[Fe(TPP)(*t*-BuNC)$_2$]$^+$	2.12	0.13	120	44
[Fe(TMP)(2-MeHIm)$_2$]$^+$	1.48	0.20	77	45
[Fe(TMP)(3-EtPy)$_2$]$^+$	1.25	0.18	77	45
[Fe(TMP)(3-ClPy)$_2$]$^+$	1.36	0.20	77	45
[Fe(TMP)(4-NMe_2Py)$_2$]$^+$	1.75	0.18	4.2	46
[Fe(TMP)(1,2-Me_2Im)$_2$]$^+$	1.25	0.14	250	47
	1.26	0.17	120	47
[Fe(TPP)(4-CNPy)$_2$]$^+$	0.65	0.19	120	48
[Fe(TPP)(Py)$_2$]$^+$	1.25	0.16	77	49
[Fe(TPP)(2-MeHIm)$_2$]$^+$	1.77	0.22	150	50
[Fe(TMP)(1-MeIm)$_2$]$^+$	2.31	0.28	4.2	46
[Fe(OEP)(4-NMe_2Py)$_2$]$^+$	2.15	0.26	4.2	46
[Fe(T*p*-OCH_3PP)(HIm)$_2$]$^+$	2.06	0.17	298	51
[Fe(T*p*-ClPP)(HIm)$_2$]$^+$	2.01	0.15	298	51
[(PPh(OMe)$_2$)$_2$Fe(T(*p*-Me)PP)]CF_3SO_3	1.23	0.35	80	53
MbCN	1.46	0.16	4.2	54
CCPCN	1.60	0.21	4.2	54
Fe(II) Complexes				
[Fe(TpivPP)(NO_2)(NO)]$^-$ (form 1)	1.78	0.22	200	15
[Fe(TpivPP)(NO_2)(NO)]$^-$ (form 2)	1.20	0.35	4.2	15
[Fe(TPP)(NO)]	1.24	0.35	4.2	15
[Fe(OEP)(NO)]	1.26	0.35	100	52
[Fe(TpivPP)(NO_2)]$^-$	2.28	0.41	4.2	12

[a] This work.

orientations.[45−50] In these systems, the symmetrical interaction of the two ligands rotated by 90° leads to the near-equivalence of the two d_π orbitals and Mössbauer quadrupole splittings less than 1.75 mm/s.[46,58] In addition for [Fe(Porph)(NO_2)(NO)], the asymmetry parameter, η, has been found to have the relatively small value of 0.25; this value must result from near-equivalence of the d_π orbitals. For the [Fe(Porph)(NO_2)(NO)] systems, such a near-equivalence of the d_π orbitals must result from the interaction of the linear nitrosyl ligand and not the nitrite. Indeed, earlier Mössbauer work on iron(nitro) complexes has made clear that the effects of the axial nitro ligand is to increase the energy gap between the two d_π orbitals.[12] The increased gap results since the nitrite ion can interact with only one of the d_π's.

The data of Table 5 demonstrate that smaller isomer shifts for iron(III) porphyrinates result when the axial ligands are strong π acceptors such as the isocyanide complexes[44] or nitric oxide. An interesting comparison of the isomer shift for the five-coordinate iron(III) nitric oxide derivative and the six-coordinate nitrite complexes can be made. Two N-bound nitrite ions or N-bound nitrite and another axial ligand do not have a significant influence on decreasing the isomer shift from the usual values seen for low-spin iron(III). The nitrosyl complex, on the other hand, does have a decreased value of the isomer shift but that of the mixed (nitro)(nitrosyl) complex is decreased even more. Thus, both the observed isomer shifts and the quadrupole splittings suggest that the [Fe(Porph)(NO_2)(NO)] species are derivatives in which the iron(III) center strongly π donates to the two axial ligands. Further, if the isomer shift truly reflects the π bonding in the system, there must be a synergic effect of the two axial ligands on the magnitude of the π donation of iron. The apparent near-equivalence of the energy of the two d_π orbitals must reflect the dominance of nitric oxide in the bonding.

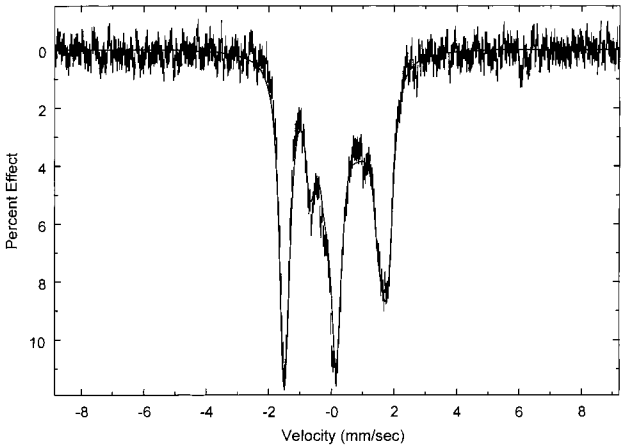

Figure 5. Mössbauer spectrum of [Fe(TPP)(NO_2)(NO)] taken at 4.2 K with an applied magnetic field of 7 T parallel to the γ-ray beam. The solid line is a diamagnetic fit to the data which yields the following parameters: quadrupole splitting, $\Delta E_q = +1.36$ mm/s; asymmetry parameter, $\eta = 0.25$; isomer shift, $\delta_{Fe} = 0.15$ mm/s; and Lorentzian width γ (fwhm) = 0.33 mm/s.

Finally, we turn to the magnetic properties and the electronic state of the {FeNO}^{6} unit. Westcott and Enemark[59] have enumerated nine possible descriptions of the {FeNO}^{6} unit; all but two of these are paramagnetic. The foregoing structural and spectroscopic data for the [Fe(Porph)(NO_2)(NO)] complexes are consistent with a low-spin d^5 iron(III) center. In the simplest analysis of the systems, the compounds would be diamagnetic if the d^5 center is antiferromagnetically coupled to the $S = {}^1/_2$ nitrosyl or paramagnetic if the coupling is ferromagnetic; four additional possible coupling models with a d^5 center are also paramagnetic. Our Mössbauer measurements in an applied magnetic field (4.2 K) show, quite clearly, that the ground state of [Fe(TPP)(NO_2)(NO)] is diamagnetic. The experimental spectrum and the diamagnetic fit obtained are shown in Figure 5. Completely adequate fits for the Mössbauer measurements obtained in applied field for [Fe(T*p*-OCH_3PP)(NO_2)(NO)] and [Fe(TpivPP)(NO_2)(NO)] could not be obtained because of the presence of impurities in the bulk samples. Nonetheless, the observed narrow lines are consistent with diamagnetic ground states. However, Settin and Fanning[18] have measured the magnetic susceptibility of [Fe(TPP)(NO_2)(NO)]·C_7H_8·$2H_2O$ and observed a room-temperature moment of 1.5 μ_B. Moreover, the

(56) Almost all low-spin iron porphyrinate systems display an EPR spectrum, and the *g* values can be used to calculate the relative orbital energies of the three lowest orbitals in terms of the value of the spin−orbit coupling constant. This is conveniently done with the Taylor formulation.[57]

(57) Taylor, C. P. S. *Biochim. Biophys. Acta* **1977**, *491*, 137.
(58) Medhi, O. K.; Silver, J. *J. Chem. Soc., Dalton Trans.* **1990**, 555.
(59) Westcott, B. L.; Enemark, J. H. In *Inorganic Electronic Structure and Spectroscopy*; Lever, A. B. P., Solomon, E. I., Eds.; Wiley and Sons: New York, in press.

related complex $[Fe(OEP)(NO)]^+$ also displayed paramagnetism at room temperature.[9] These nonzero room-temperature magnetic moments suggest the possibility of paramagnetic excited states in $\{FeNO\}^6$ systems. The meaning of these interesting observations are tempered, however, by our recognition of the difficulties of obtaining pure samples in large enough quantity to carry out bulk measurements.

We have examined the temperature-dependent magnetic susceptibility for a sample of $[Fe(OEP)(NO_2)(NO)]$ in order to determine if these systems exhibit some excited state leading to a magnetic moment. We carried out measurements on the OEP derivative since that sample had shown the smallest amount of an iron(II) nitrosyl impurity in bulk preparations. Our measurements (6−300 K) show paramagnetism, although the absolute magnitude (0.8−0.9 μ_B) is smaller than that reported earlier. There is little temperature dependence over the 6−300 K temperature range examined with a slight decrease in the observed moment above 250 K. The slight decrease in the susceptibility is in the opposite direction from that expected if a paramagnetic excited state is responsible for the moment. IR data for the sample suggests an apparent, but small, iron(II) nitrosyl impurity. The solid state sample used for the susceptibility measurements displays an EPR spectrum that bears some resemblance to, but is not the spectrum of, a pure iron(II) nitrosyl. Hence we originally thought the EPR signal might arise from an excited state. However, single-crystal EPR measurements for a sample of $[Fe(OEP)(NO_2)(NO)]$ showed that the EPR signal had similar rotational behavior to a dilute solid-state solution of [Fe(OEP)(NO)] in [Co(OEP)(NO)]. Moreover, the 77 K solution state spectrum of a freshly prepared (in situ) sample showed no EPR signal. Although the issue of impurities in samples of $[Fe(Porph)(NO_2)(NO)]$ is a difficult one, we conclude that there is no low-lying excited state that yields the observed magnetic moment and that the observed susceptibility arises from the presence of a paramagnetic nitrosyl impurity.

Summary. The synthesis and structural characterization of several $[Fe(Porph)(NO_2)(NO)]$ derivatives are reported. Two new synthetic methods have been successfully executed and crystalline species isolated and characterized by X-ray structure analysis and Mössbauer spectroscopy. For two picket fence porphyrin derivatives, the two similarly sized axial ligands are differentiated in the solid-state structures. Both axial Fe−N distances are slightly longer than those found in related derivatives where nitrosyl or nitrite is the only nitrogen oxide ligand. The NO does not exert a significant structural trans effect in these iron(III) derivatives. The $[Fe(Porph)(NO_2)(NO)]$ derivatives clearly have a diamagnetic ground state and we have no evidence for the presence of a thermally accessible paramagnetic excited state.

Acknowledgment. We thank T. J. Neal for assistance with the magnetic susceptibility measurements and Prof. R. G. Hayes for single-crystal EPR measurements. We thank the National Institutes of Health for support of this research under Grant GM-38401 to W.R.S. and GM-48513 to C.E.S. Funds for the purchase of the FAST area detector diffractometer were provided through NIH Grant RR-06709, and funds for the SQUID susceptometer, by NSF Grant DMR-9703732 to the University of Notre Dame.

Supporting Information Available: Tables S1−S30, with complete crystallographic details, atomic coordinates, bond distances and angles, anisotropic temperature factors, and fixed hydrogen atom positions for all five structures; Figures S1−S4, with formal diagrams of the porphinato core for $[Fe(T\textit{p}\text{-}OCH_3PP)(NO_2)(NO)]$ and $[Fe(TpivPP)(NO_2)(NO)]$ (**1**, **2**, and **3**); and Figures S5−S9, which include ORTEP drawings of $[Fe(T\textit{p}\text{-}OCH_3PP)(NO_2)(NO)]$ and $[Fe(TpivPP)(NO_2)(NO)]$ (**1**, **2**, **3**, and **4**) (55 pages). Ordering information is given on any current masthead page.

IC981162N